Quantitative Characterization of Polymer-Polymer, Protein-Protein, and Polymer-Protein Interaction via Tracer Sedimentation Equilibrium

ARTICLE *in* THE JOURNAL OF PHYSICAL CHEMISTRY B · AUGUST 2010

Impact Factor: 3.3 · DOI: 10.1021/jp104342f · Source: PubMed

2 AUTHORS:

Adedayo Akinkunmi Fodeke
Obafemi Awolowo University
8 PUBLICATIONS **45** CITATIONS

SEE PROFILE

Allen P Minton
National Institutes of Health
168 PUBLICATIONS **10,732** CITATIONS

SEE PROFILE

Published in final edited form as:
J Phys Chem B. 2010 August 26; 114(33): 10876–10880. doi:10.1021/jp104342f.

Quantitative Characterization of Polymer–Polymer, Protein–Protein, and Polymer–Protein Interaction via Tracer Sedimentation Equilibrium

Adedayo A. Fodeke[†] and **Allen P. Minton**[*]
Section on Physical Biochemistry, Laboratory of Biochemistry and Genetics, National Institute of Diabetes and Digestive and Kidney Diseases, National Institutes of Health, U.S. Department of Health and Human Services, Bethesda, Maryland 20892

Abstract

Quantitative analysis of the composition dependence of the concentration gradient of each species of macromolecule within a solution mixture at sedimentation equilibrium permits the quantitative characterization of self- and heterointeractions between sedimenting solutes. Sedimentation equilibrium experiments were conducted on solutions containing a trace concentration of FITC-labeled BSA in varying concentrations of Ficoll 70 and on solutions containing a trace concentration of FITC-labeled Ficoll 70 in varying concentrations of BSA. The equilibrium gradient of each solute component in each mixture was measured independently. Analysis of the resulting gradients resulted in evaluation of the dependence of the activity coefficient of Ficoll upon the concentrations of Ficoll and BSA at concentrations of up to 100 g/L and the dependence of the activity coefficient of BSA upon the concentrations of Ficoll and BSA at concentrations of up to 100 g/L. The activity coefficients of both species increase significantly with increasing Ficoll and BSA concentration and do not vary with temperature, to within the precision of measurement, over the temperature range of 5–37 °C, indicating that the dominant interaction between Ficoll molecules and between BSA and Ficoll molecules is repulsive and probably due to steric volume exclusion. The measured dependences may be accounted for quantitatively by a simple model in which BSA and Ficoll 70 are represented by equivalent rigid particles.

Introduction

The detection and characterization of noncovalent interactions between biological macromolecules is a widespread and cross-disciplinary goal of research in biochemistry, biophysics, and cell biology. Although one often finds the term “interaction” used interchangeably with “complex formation”, not all intermolecular interactions result in the formation of stable complexes. Nonspecific weakly attractive and repulsive intermolecular interactions, although usually undetectable in dilute solution, are increasingly recognized as having a substantial effect upon macromolecular stability, structure, and function in highly concentrated or volume-occupied (“crowded”) solutions resembling physiological fluid media.[1,2] In the present work, the interaction between two species of macromolecules (*i* and *j*) is quantified as the dependence of the free energy of solvation of species *i*, $\Delta G_{\mathrm{solv},i}$, or the logarithm of the thermodynamic activity coefficient, γ_i, on the concentration of species *j*. If $d\Delta G_{\mathrm{solv},i}/dc_j = d\ln \gamma_i/dc_j$ is negative under a certain set of experimental conditions, the interaction between species *i* and *j* is net attractive under those conditions, and if $d\Delta G_{\mathrm{solv},i}/dc_j$ is positive, the interaction between species *i* and *j* is net repulsive.

[*]To whom correspondence should be addressed: minton@helix.nih.gov.
[†]Permanent address: Department of Chemistry, Obafemi Awolowo University, Ile-Ife, Nigeria.

The present study is aimed at the quantitative characterization of self-interaction between molecules of a model polysaccharide, Ficoll 70 (Ficoll), self-interaction between molecules of a model protein, bovine serum albumin (BSA), and heterointeraction between molecules of Ficoll and BSA in saline solution at neutral pH. Measurements were carried out in moderately saline solutions at neutral pH containing arbitrarily large concentrations of Ficoll and a trace concentration of BSA and in solutions containing arbitrarily large concentrations of BSA and a trace concentration of Ficoll. The activity coefficients of each species were measured as functions of the concentrations of both species utilizing the method of nonideal tracer sedimentation equilibrium.[3] Following presentation of the results, an approximate statistical thermodynamic model is presented that accounts quantitatively for the observed dependence of the experimentally observed concentration gradients upon Ficoll and BSA concentration.

Materials and Experimental Methods

Materials

Ficoll 70 and bovine serum albumin (reagent grade lyophilized powder 98% monomer) were obtained from Sigma-Aldrich (St. Louis, MO). Both were used without further purification. BSA and Ficoll 70 were equilibrated with phosphate-buffered saline (0.05 M sodium phosphate and 0.15 M NaCl at pH 7.4) by extensive dialysis. Labeling of protein and amidated Ficoll with fluorescein isothiocyanate (FITC) was performed using an EZ-Label protein labeling kit (Pierce, Rockford, IL).

Labeling of BSA with Fluorescein Isothiocyanate (FITC)

Labeling was carried out according to instructions provided with the EZ-Label kit, with slight modification. An approxmately 15-fold molar excess of FITC was dissolved in 2 mL of 10 mg/mL BSA in borate buffer pH 8.6. The reacting mixture was allowed to incubate in the dark at room temperature for 2 h. Excess hydrolyzed FITC was removed by passing the mixtures of labeled protein and excess FITC through a dextran desalting column provided with the labeling kit and dialyzing extensively against phosphate-buffered saline. To determine whether the labeling had perturbed the BSA, samples of both labeled and unlabeled protein were chromatographed on a Superdex 200 size exclusion column (GE Healthcare Biosciences, Uppsala). The extent of labeling, as determined by measurement of absorbance at 280 and 500 nm, was approximately 2 mol FITC/mol BSA. Eluting peaks were monitored by light scattering and refractometric flow detectors (Wyatt Technology, Santa Barbara, CA) and analyzed to yield the molecular weight of each sample, which was found to be identical to within experimental uncertainty for the labeled and unlabeled protein.

Labeling of Ficoll 70 with FITC

Ficoll was amidated as described.[4] Ficoll 70 (1.33 g) was dissolved in 18.5 mL of freshly prepared 1.35 M sodium chloroacetate. Five milliliters of 10 M NaOH was then added, and the reaction mixture was brought to 25 mL with distilled water. After 45 min at 25 °C, the reaction was quenched with 0.2 M NaH_2PO_4, and the mixture was titrated with ca. 9.5 mL of 6 M HCl to pH 7.0. The activated Ficoll 70 was then dialyzed for 3 days against distilled water, then lyophilized and resuspended in distilled water at a concentration of 25 mg/mL. Ethylenediamine dihydrochloride was added at 5.7 mg/mg of Ficoll 70 while a constant pH of 4.7 was maintained with 1 M sodium hydroxide. Next, 0.5 mg/mg of 1-ethyl-3-(3-dimethylaminopropyl)carbodiimide was added over a 10 min period, and the mixture was stirred for 3.5 h at room temperature while the pH was maintained at 4.7–6.0. The amidated Ficoll 70 was dialyzed extensively against distilled water, lyophilized, and resuspended in borate buffer pH 8.6. FITC labeling of the amidated polymer was done essentially as

described above for the protein, except that excess hydrolyzed FITC was removed by extensive dialysis for several days in phosphate buffer pH 7.4. The degree of labeling of the Ficoll was determined by measuring the concentrations of FITC via absorbance (ε_{495}^{1cm}=72 000 M^{-1}) and Ficoll by differential refractometry (dRI/dw_{fic} = 0.141 cm^3/g). The ratio of the two concentrations so determined was found to be ca. 3 mol of FITC per mol of Ficoll 70 (calculated assuming M_{fic} = 70 000).

Tracer Sedimentation Equilibrium

Sedimentation equilibrum experiments were carried out as described in ref 5, with minor variation noted below. A solution (70 μL) containing 2 mg/mL FITC-BSA or FITC-Ficoll and either unlabeled Ficoll or BSA over a range of concentrations (5–100 mg/mL) was layered over 80 μL of fluorocarbon FC-47 (3M, St. Paul, MN) in a cylindrical polycarbonate centrifuge tube (Beckman-Coulter P/N 343775) with an inner diameter of 4.5 mm. The samples were then centrifuged in a TLS-100 swinging bucket rotor (Beckman-Coulter, Brea, CA) at rotor speeds between 10 000 and 15 000 rpm and temperatures specified below for a length of time (typically 48 h) sufficient for all solute species to attain sedimentation–diffusion equilibrium, as determined by prior test experiments. After termination of centrifugation under conditions that do not perturb the equilibrium gradient,[5] centrifuged solutions were subsequently fractionated into aliquots corresponding to 0.2 mm of radial distance r using a FR-115 microfractionator (BRANDEL, Gaithersburg, MD) as described in ref 5. The concentration of dilute FITC-labeled tracer in each fraction was measured by absorbance at 500 nm in a Spectramax 250 spectrophotometric plate reader (Molecular Devices, Sunnyvale, CA). The concentration of unlabeled BSA in each fraction was measured by absorbance at 280 nm, and the concentration of unlabeled Ficoll was measured by refractometry at 589 nm, using an Arias 500 Abbe refractometer (Reichert Instruments, Buffalo, NY). The apparent buoyant molar mass of tracer and unlabeled species in each solution was obtained by a linear least-squares fit of the natural logarithm of the relative concentration of that species as a function of the square of the radial distance according to the following equation:[3]

$$M_{i,app}^{*} = \frac{2RT}{\omega^2}\frac{d\ln S_i}{dr^2} \quad (1)$$

where R denotes the molar gas constant, T the absolute temperature, ω the angular velocity in s^{-1}, r the radial distance in cm, and S_i the signal, or measured quantity (absorbance or differential refractive index) proportional to concentration, of species i. Typical equilibrium gradients of labeled and unlabeled solutes measured by absorbance and refractometry, respectively, are plotted in Figure 1A,B.

Results

The dependence of the apparent buoyant masses of each species upon the concentration of each unlabeled species is plotted in Figure 2A–D. In all cases, the apparent buoyant mass of tracer decreases monotonically with increasing concentration of unlabeled species, indicating that self- and heterointeractions are predominantly repulsive.[3] Moreover, in Figure 2A,B, the dependence of the apparent buoyant mass of either Ficoll or FITC-BSA upon the concentration of Ficoll is seen to be independent of temperature over the range of 5–37 °C. This result indicates that self- and heterointeractions in Ficoll solutions and in Ficoll–BSA mixtures are predominantly entropic in nature and probably attributable to excluded volume. The statistical thermodynamic model presented below is based upon the

assumption that interactions between species are essentially entirely due to excluded volume.

Composition Dependence of Activity Coefficients

The general theory of sedimentation equilibrium states that the apparent buoyant mass of a particular species depends upon its interactions with all solute species present in solution and the radial concentration gradients of each of those species:[3]

$$M^*_{i,\mathrm{app}} = M^*_i - \sum_j w_j \left(\frac{d\ln\gamma_i}{dw_j}\right) M^*_{j,\mathrm{app}} \quad (2)$$

where w_j denotes the w/v concentration of solute species j. M^*_i, the limiting value of $M^*_{i,\mathrm{app}}$ in the absence of solute–solute interaction, denotes the actual buoyant mass of solute species i:

$$M^*_i = M_i \left(\frac{d\rho}{dw_i}\right)_\mu \quad (3)$$

where M_i is the actual molar mass and $(d\rho/dw_i)_\mu$ denotes the specific density increment of solute species i measured under conditions such that the chemical potential of all other solute species is held constant, that is, at dialysis equilibrium.[6] In the special case $j = i$, eq 2 reduces to the textbook relation[7]

$$M^*_{i,\mathrm{app}} = \frac{M^*_i}{1 + w_i(d\ln\gamma_i/dw_i)} \quad (4)$$

In subsequent notation, the subscript 1 will refer to Ficoll 70 and the subscript 2 will refer to BSA. In order to model the experimentally measured dependence of $M^*_{1,\mathrm{app}}$ and $M^*_{2,\mathrm{app}}$ upon w_1 and w_2, functions describing the dependence of $w_j(d\ln\gamma_i/dw_j)$ upon w_1 and w_2 are required. Two approaches will be presented below. The first is an empirical analysis based upon a power series expansion of the activity coefficients. The second is an approximate statistical thermodynamic model employing simplified descriptions of the physical properties of Ficoll and BSA molecules in solution.

Expansion of Activity Coefficients in Powers of Solute Concentration

In general, the logarithm of the activity coefficient of a solute may be expanded in powers of the concentration of all solutes:[8]

$$\ln\gamma_i = \sum_j B_{ij} w_j + \sum_j \sum_k B_{ijk} w_j w_k + \ldots \quad (5)$$

where B_{ij} denotes a coefficient of two-body interaction between molecules of species i and j, B_{ijk} a coefficient of three-body interaction between molecules of species i, j, and k, and so forth. According to the solution theory of MacMillan and Mayer,[9] the coefficients of interaction are calculable functions of the potentials of mean force acting between two, three, and higher numbers of solute molecules. In the present work, we shall be analyzing four sets of experimental results:

1. The dependence of the apparent buoyant mass of Ficoll upon Ficoll concentration (Figure 2A). Since the concentration of BSA is negligible, eq 5 reduces to

$$\ln\gamma_1 = B_{11}w_1 + B_{111}w_1^2 + \ldots \quad (6)$$

and eq 4 reduces to

$$M^*_{1,\mathrm{app}} = \frac{M^*_1}{1 + B_{11}w_1 + 2B_{111}w_1^2 + \ldots} \quad (7)$$

2. The dependence of the apparent buoyant mass of dilute BSA upon Ficoll concentration (Figure 2B). Since the concentration of BSA is negligible, eq 5 reduces to

$$\ln\gamma_2 = B_{21}w_1 + B_{211}w_1^2 + \ldots \quad (8)$$

and eq 2 reduces to

$$M^*_{2,\mathrm{app}} = M^*_2 - (B_{21}w_1 + 2B_{211}w_1^2 + \ldots)M^*_{1,\mathrm{app}} \quad (9)$$

3. The dependence of the apparent buoyant mass of BSA upon BSA concentration (Figure 2C). Since the concentration of Ficoll in these experiments is negligible, eq 5 reduces to

$$\ln\gamma_2 = B_{22}w_2 + B_{222}w_2^2 + \ldots \quad (10)$$

and eq 4 reduces to

$$M^*_{2,\mathrm{app}} = \frac{M^*_2}{1 + B_{22}w_2 + 2B_{222}w_2^2 + \ldots} \quad (11)$$

4. The dependence of the apparent buoyant mass of dilute Ficoll upon BSA concentration (Figure 2D). Equation 5 reduces to

$$\ln\gamma_1 = B_{12}w_2 + B_{122}w_2^2 + \ldots \quad (12)$$

and eq 2 reduces to

$$M^*_{1,\mathrm{app}} = M^*_1 - (B_{12}w_2 + 2B_{122}w_2^2 + \ldots)M^*_{2,\mathrm{app}} \quad (13)$$

Equations 7, 9, 11, and 13 were used to simultaneously model the data corresponding to cases 1–4 listed above, to obtain best fit values of M^*_1=23 200 ± 1500, M^*_2=17 800 ± 1200, B_{11} = 27.9 ± 14 mL/g, B_{22} = 15.6 ± 8 mL/g, B_{12} (= B_{21}) = 21.3 ± 7 mL/g, B_{111} = 178 ± 120 (mL/g)2, B_{222} = 83.1 ± 60 (mL/g)^2, B_{211} = 96.7 ± 70 (mL/g)2, and B_{122} = 84.7 ± 45 (mL/g)2, where the indicated uncertainties correspond to ± one standard error of estimate. The dependence of the apparent buoyant masses of Ficoll 70 and BSA upon solution composition, calculated using these equations and best-fit parameter values, is plotted (solid curves) together with each of the corresponding data sets in Figure 2A–D. The dependence of $\Delta\Delta G_{\mathrm{solv,fic}} = RT\ln\gamma_{\mathrm{fic}}$ and $\Delta\Delta G_{\mathrm{solv,BSA}} = RT\ln\gamma_{\mathrm{BSA}}$ upon the concentrations of both species, calculated using eqs 6, 8, 10, and 12 together with the best-fit values of the B_{ij} and

B_{ijk} is plotted in Figure 3A,B. Ficoll–Ficoll interactions are seen to be the most repulsive, Ficoll–BSA interactions less repulsive, and BSA–BSA interactions the least repulsive, qualitatively in accord with our expectation that Ficoll has a larger volume of exclusion per unit mass than BSA.

Effective Hard Convex Particle Model for Protein–Protein, Polymer–Polymer, and Polymer–Protein Interaction

The experimentally measured concentration dependence of several colligative properties of concentrated solutions of BSA and concentrated mixtures of BSA and other proteins has been successfully described by relations derived from theories of hard particle fluids.[10–13] For this purpose, each protein molecule is represented as an equivalent hard sphere, the volume of which reflects not only the actual size of the molecule but also additional "soft" repulsions.[1,13]

Here we introduce an extension of this model to mixtures of BSA and Ficoll 70. Ficoll 70 is a highly cross-linked, nonionic polymer of glucose. Measurements of dynamic light scattering and membrane transport suggest that Ficoll has a structure that is intermediate between that of a globular protein and a random coil polymer[14] and may exhibit significant deviations from sphericity.[15] In our simplified model, we represent a molecule of Ficoll by an equivalent spherocylinder of specific volume v_{fic} and axial ratio L_{fic}, defined as the ratio of the length of the cylindrical region to its diameter. (A sphere is a special case of a spherocylinder with $L = 0$.) The specific volume of the equivalent sphere representing BSA depends upon the nature of the molecule with which it is interacting. In saline solution, BSA carries significant negative charge at neutral pH,[13] and due to the presence of repulsive electrostatic interactions between BSA molecules, the size of the effective sphere representing BSA for the purpose of estimating self-interaction is expected to be different (and larger) than the size of the effective sphere representing BSA for the purpose of estimating interaction with the nonionic polymer. We will denote these two specific volumes by $v_{BSA,BSA}$ and $v_{BSA,fic}$, respectively.

By representing each species of macromolecule by an equivalent hard convex particle (i.e., sphere or spherocylinder), the activity coefficient of each macromolecular solute in a fluid mixture of solute species at arbitrary concentration may be estimated using the scaled particle theory (SPT) of hard convex particle mixtures.[16] SPT calculations were performed using expressions provided in the Appendix of ref 17. Actual and buoyant molar masses are related by eq 3, where the value of the density increment $(d\rho/dw)_\mu$ is taken as 0.27 for BSA and 0.38 for Ficoll.[18]

The four sets of experimental data listed in the preceding section were analyzed in the context of the effective hard convex particle model as follows:

1. The dependence of $M^*_{fic,app}$ upon Ficoll concentration (Figure 2A) is calculated using eq 4, with $d\ln \gamma_1/dw_1$ calculated using SPT with $v_1 = v_{fic}$.
2. The dependence of $M^*_{FITC-BSA,app}$ upon Ficoll concentration (Figure 2B) is calculated using eq 2; $d\ln \gamma_2/dw_1$ is calculated using SPT with $v_1 = v_{fic}$ and $v_2 = v_{BSA,fic}$. $M^*_{fic,app}$ is calculated as described in the preceding paragraph.
3. The dependence of $M^*_{FITC-BSA,app}$ upon BSA concentration (Figure 2C) is calculated using eq 4; $d\ln \gamma_2/dw_2$ is calculated using SPT with $v_2 = v_{BSA,BSA}$.

4. The dependence of $M^*_{FITC-fic,app}$ upon BSA concentration (Figure 2D) is calculated using eq 2; $d\ln \gamma_1/dw_2$ is calculated using SPT with $v_1 = v_{fic}$ and $v_2 = v_{BSA,fic}$. $M^*_{BSA,app}$ is calculated as described in the preceding paragraph.

The calculated dependence of the apparent buoyant masses of Ficoll 70 and BSA upon solution composition, calculated using these equations together with the best-fit values of the parameters M_{fic} = 59 100 ± 3000, M_{BSA} = 64 600 ± 3000, v_{fic} = 1.3 ± 0.7 mL/g, L_{fic} = 6.6 (−4, + 8), $v_{BSA,fic}$ = 1.6 ± 0.2 mL/g, and $v_{BSA,BSA}$ = 1.9 ± 0.3 mL/g, where the indicated uncertainy corresponds to ± one standard error of estmate, is plotted (dashed curves) together with each of the corresponding data sets in Figure 2A–D.

Discussion

The experimental technique employed in the present study— nonideal tracer sedimentation equilibrium—provides a quantitative measure of the free energy of interaction between a test solute molecule and molecules of the same or another solute species at arbitrary concentration. The effective hard sphere model best describing the concentration dependence of the equilibrium gradient of BSA is in semiquantitative agreement with that describing concentration-dependent light scattering under comparable conditions,[10] thus validating the present implementation of the technique as well as providing additional confirmation of the broad applicability of the effective hard sphere approximation.[11] The present work provides the first measurement of the free energy of polymer–protein and polymer–polymer interactions at concentrations up to 100 g/L. We have utilized nonideal tracer sedimentation equilibrium to demonstrate that, to within the precision of measurement, the free energy of interaction between Ficoll and Ficoll and between Ficoll and BSA is positive and independent of temperature between 5 and 37 °C. This result indicates that, over this temperature range, interactions between Ficoll and Ficoll and between Ficoll and BSA are net repulsive and predominantly entropic in nature and hence presumed to be due primarily to volume exclusion.

The combined data are well described by an empirical expansion of the logarithm of the activity coefficient of each trace species in powers of the concentration of the abundant species, truncated after the quadratic terms. This finding is consistent with the observation that the logarithm of the activity coefficient of hemoglobin in hemoglobin solutions can be quantitatively described by a power series truncated after quadratic terms at concentrations up to ca. 100 g/L.[19] The empirical description requires specification of the buoyant molar mass of Ficoll (species 1) and BSA (species 2) and seven two- and three-body interaction coefficients. The combined data are equally well accounted for by a simplified effective hard convex particle model employing only four structural parameters. According to this model, BSA is best described as a sphere with a diameter of ca. 69 Å, and Ficoll is best described as a moderately elongated particle (spherocylinder) with an cylindrical axial ratio of ca. 7, corresponding to a diameter of ca. 28 Å and an end-to-end length of ca. 184 Å. This conclusion is semiquantitatively consistent with the observation that the intrinsic viscosity of Ficoll 70 is approximately 3 times greater than that of a typical globular protein[7,20] since an ellipsoid of rotation with an axial ratio of about 7 is predicted to exhibit an intrinsic viscosity approximately 3 times that of a spherical particle of equal volume.[7] In addition, the ability of Ficoll to pass through nanoporous membranes significantly more rapidly than a globular protein of equal mass has been attributed to shape asymmetry.[15] In Figure 4, the best-fit effective sphere representing BSA is superimposed upon the crystallographically determined atomic structure of human serum albumin,[21] which is thought to have a solution structure very similar to that of uncrystallizable BSA.[22] It is evident that the volumes excluded by the equivalent sphere and the atomic model to particles of comparable size are quite similar, supporting our model assumption that the interaction between charged BSA and uncharged

Ficoll at neutral pH, in contrast to the interaction between two charged molecules of BSA, is due predominantly to steric exclusion. The best-fit effective hard convex particle model thus not only provides a parsimonious description of the extensive body of data reported here but also provides a physically meaningful low-resolution description of molecular size and shape and intermolecular interactions in highly nonideal solution.

Acknowledgments

The authors thank Cristina Fernández (NIH) for assistance with chromatographic characterization, and Peter McPhie (NIH) for critical review of a draft of this report. This research was supported by the Division of Intramural Research, National Institute of Diabetes and Digestive and Kidney Diseases.

References and Notes

1. Hall D, Minton AP. Biochem Biophys Acta. 2003; 1649:127. [PubMed: 12878031]
2. Zhou HX, Rivas G, Minton AP. Annu Rev Biophys. 2008; 37:375. [PubMed: 18573087]
3. Rivas G, Fernández JA, Minton AP. Biochemistry. 1999; 38:9379. [PubMed: 10413513]
4. Luby-Phelps K, Castle PE, Taylor DL, Lanni F. Cell Biol. 1987; 84:4910.
5. Darawshe S, Rivas G, Minton AP. Anal Biochem. 1993; 209:130. [PubMed: 8465945]
6. Eisenberg, H. Biological Macromolecules and Polyelectrolytes in Solution. Clarendon Press; Oxford: 1976.
7. Tanford, C. Physical Chemistry of Macromolecules. Wiley & Sons; New York: 1961.
8. Minton AP. Methods Enzymol. 1998; 295:127. [PubMed: 9750217]
9. McMillan WG Jr, Mayer JE. J Chem Phys. 1945; 13:276.
10. Fernández C, Minton AP. Biophys J. 2009; 96:1992. [PubMed: 19254559]
11. Minton AP. J Pharm Sci. 2007; 96:3466. [PubMed: 17588257]
12. Minton AP. Biophys J. 2008; 94:L57. [PubMed: 18212007]
13. Minton AP, Edelhoch H. Biopolymers. 1982; 21:451.
14. Fissell WH, Hofmann CL, Smith R, Chen MH. Am J Physiol Renal Physiol. 2010; 298:F205. [PubMed: 19846572]
15. Asgeirsson D, Venturoli D, Fries E, Rippe B, Rippe C. Acta Physiol. 2007; 191:237.
16. Boublík T. Mol Phys. 1974; 27:1415.
17. Minton AP. Biophys J. 2007; 93:1321. [PubMed: 17526566]
18. Durschlag, H. Specific Volumes of Biological Macromolecules and Some Other Molecules of Biological Interest. In: Hinz, HJ., editor. Thermodynamic Data for Biochemistry and Biotechnology. Springer-Verlag; Berlin: 1986.
19. Ross PD, Minton AP. J Mol Biol. 1977; 112:437. [PubMed: 875025]
20. GE Healthcare Data File 18-1158-27 AB: Ficoll PM70, Ficoll PM400. 2007
21. He XM, Carter DC. Nature. 1992; 358:209. [PubMed: 1630489]
22. Ferrer ML, Duchowicz R, Carrasco B, Garcia de la Torre J, Acuña AU. Biophys J. 2001; 80:2422. [PubMed: 11325741]

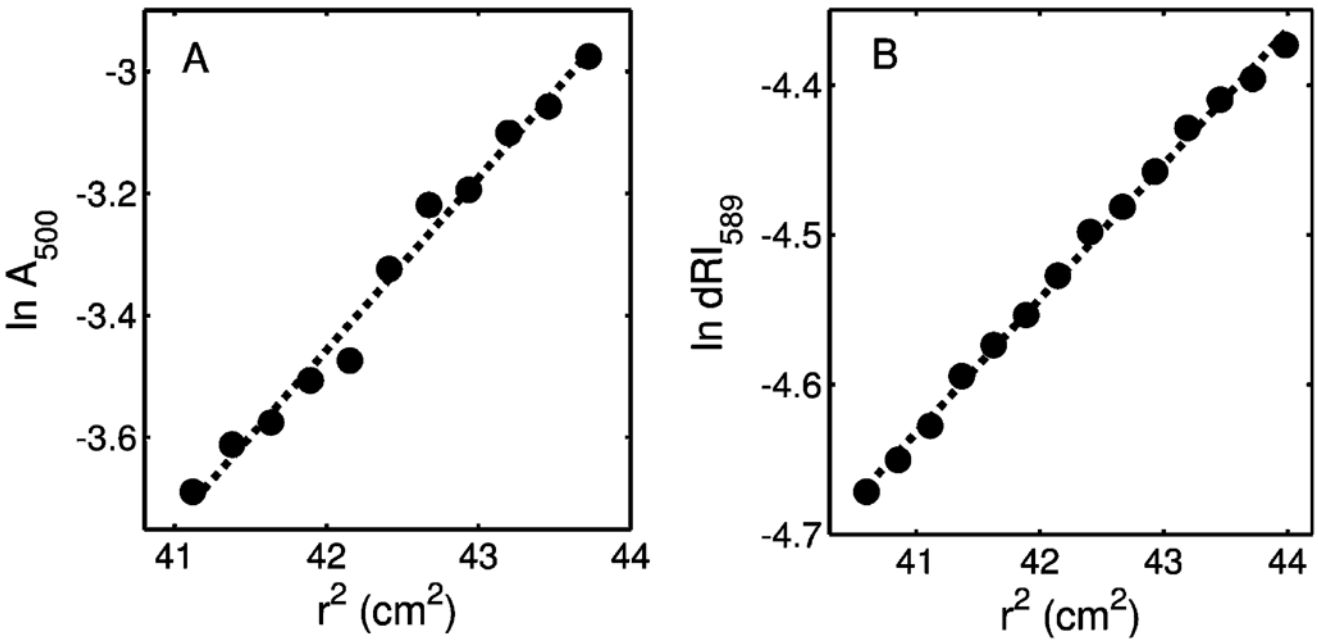

Figure 1.

Experimentally measured equilibrium gradients, linearized in accordance with eq 1. (A) Logarithm of absorbance of FITC-BSA (loading concentration 2 g/L) in Ficoll (loading concentration 10 g/L) at sedimentation equilibrium plotted against square of radial position in the centrifuge (T = 37 °C). Slope of best-fit straight line (dashed) yields $M^*_{\mathrm{BSA,app}}$=13 250. (B) Logarithm of differential refractive index of Ficoll (loading concentration 80 g/L) plotted against square of radial position in the centrifuge (T = 5 °C). Slope of best-fit straight line (dashed) yields $M^*_{\mathrm{Fic,app}}$=3800.

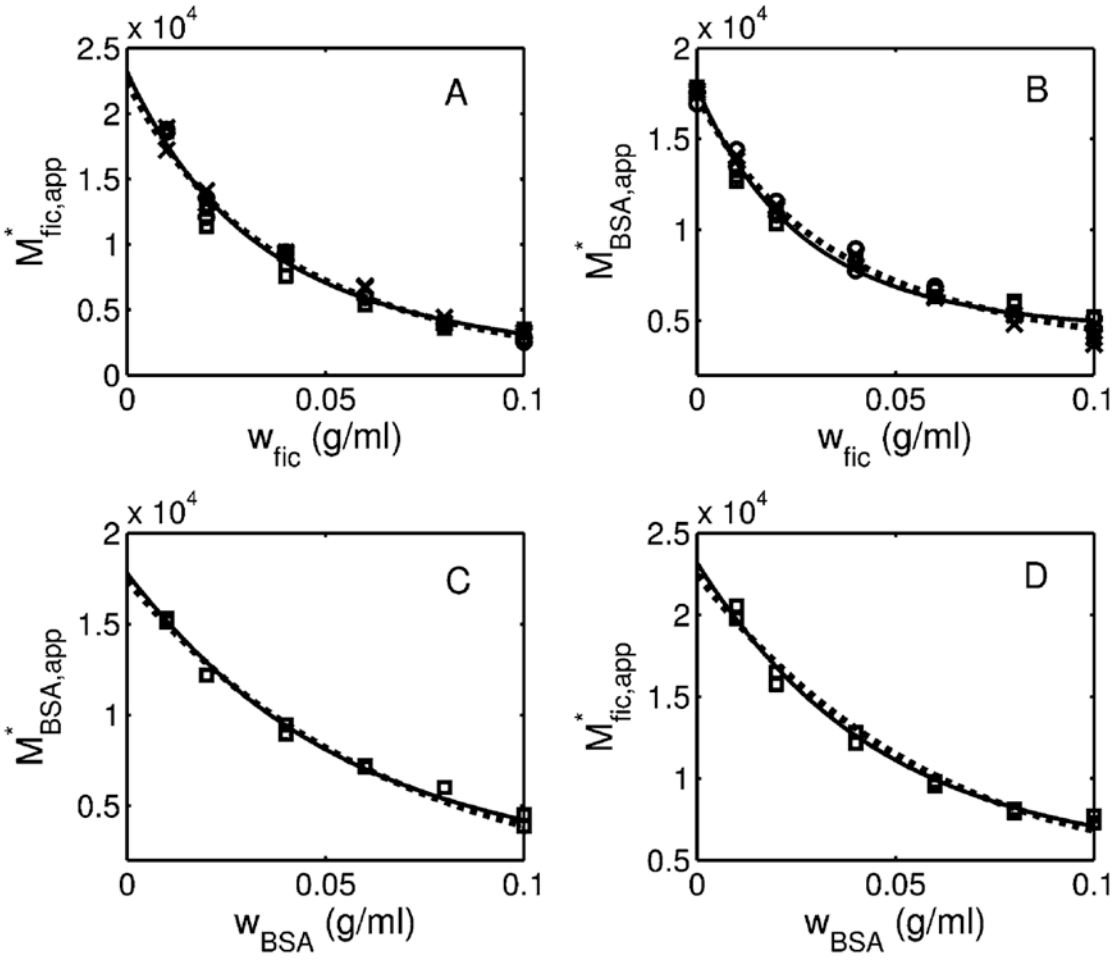

Figure 2.

Dependence of apparent buoyant molar mass upon concentration of the abundant solute. Symbols: experimental data, × −37 °C, □ −20 °C, ○ −5 °C. Solid curve: best-fit of empirical analysis. Dashed curve: best-fit of simplified hard convex particle model. (A) Ficoll in Ficoll. (B) FITC-BSA in Ficoll. (C) FITC-BSA in BSA. (D) FITC-Ficoll in BSA.

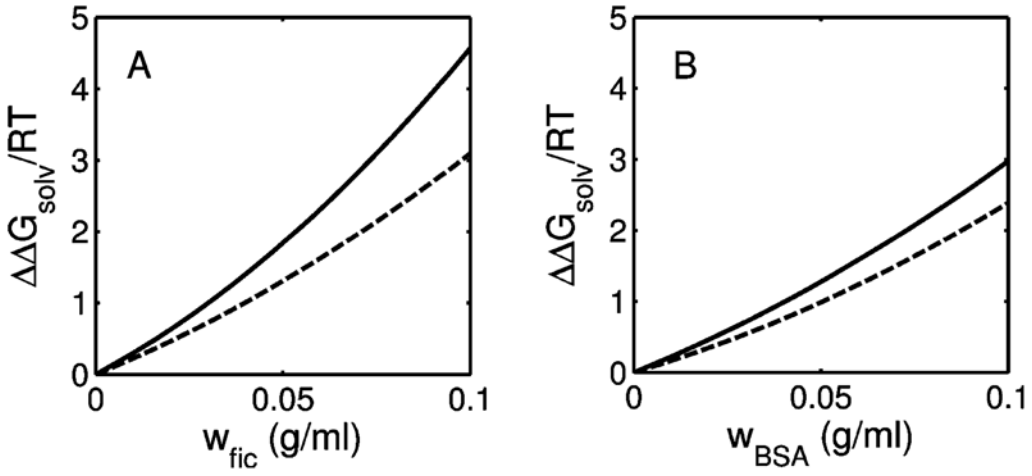

Figure 3.

Dependence of $\Delta\Delta G_{solv}/RT = \ln \gamma$ upon concentration of the abundant solute species, calculated using eqs 6, 8, 10, and 12 with best-fit values of the B_{ij} and B_{ijk} given in the text. (A) Solid line, Ficoll in Ficoll; dashed line, FITC-BSA in Ficoll. (B) Solid line, FITC-Ficoll in BSA; dashed line, FITC-BSA in BSA.

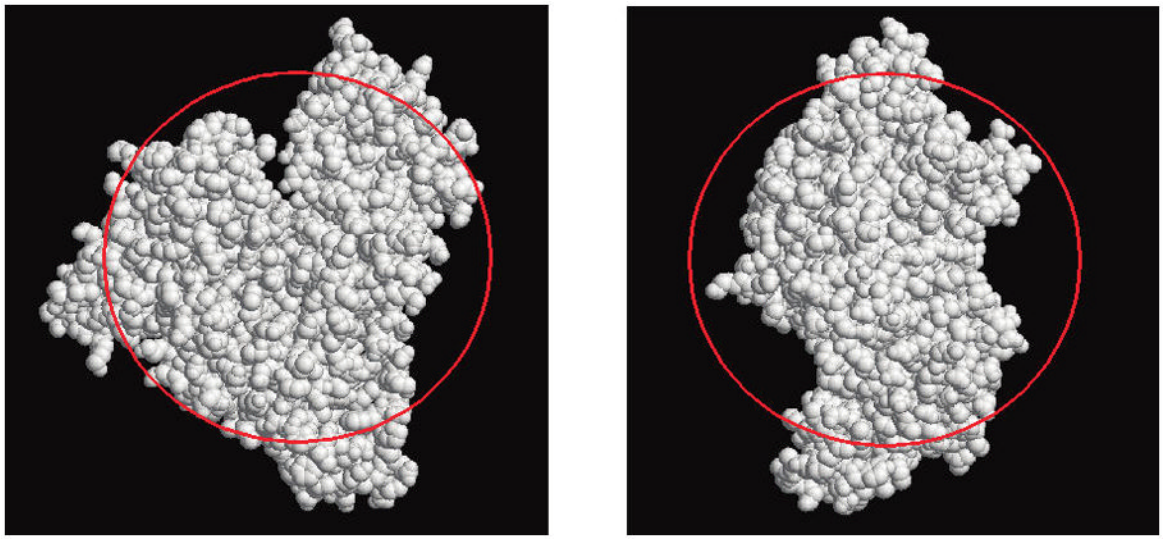

Figure 4.
Outline of a sphere of diameter 69 Å superimposed upon two projections of a space-filling model of the crystal structure of human serum albumin (PDB 1UOR).